

# Experimental proof of the feasibility of using an angled fiber-optic probe for depth-sensitive fluorescence spectroscopy of turbid media

Quan Liu and Nirmala Ramanujam

*Department of Biomedical Engineering, University of Wisconsin—Madison, 2143 Engineering Centers Building,  
1550 Engineering Drive, Madison, Wisconsin 53706*

Received March 26, 2004

An angled fiber-optic probe that facilitates depth-sensitive fluorescence measurements was developed for enhancing detection of epithelial precancers. The probe was tested on solid, two-layered phantoms and proved to be effective in selectively detecting fluorescence from different layers. Specifically, a larger illumination angle provides greater sensitivity to fluorescence from the top layer as well as yielding an overall higher fluorescence signal. Monte Carlo simulations of a theoretical model of the phantoms demonstrate that increasing the illumination angle results in an increased excitation photon density and, thus, in increased fluorescence generated in the top layer. © 2004 Optical Society of America

OCIS codes: 060.2350, 300.2530, 300.6540, 170.3660, 170.3880.

Stratified squamous epithelial tissues such as cervix, oral cavity, and skin are essentially layered structures that consist of an epithelial layer, a basement membrane, and an underlying stroma. The depth distribution of endogenous fluorophores in these tissues varies with a number of factors including age, menopausal status,<sup>1,2</sup> and disease progression (from normal to dysplasia to carcinoma).<sup>3,4</sup> Hence fiber-optic probes that facilitate depth-sensitive fluorescence spectroscopy may provide superior detection of precancers and cancers in these tissues than fiber-optic probes that volume-average the fluorescence from different sublayers. Previously a multiseparation approach (varying the separation between illumination and collection fibers) was employed for depth-resolved fluorescence detection from turbid media.<sup>5</sup> Monte Carlo modeling of this probe geometry for depth-resolved fluorescence detection from a two-layered model of epithelial tissue indicated that this probe is sensitive to the fluorescence that originates from the deeper stromal layer but not to surface epithelial fluorescence.<sup>6</sup>

Subsequently, we showed by using Monte Carlo simulations that an angled probe geometry that allows variable illumination angles of 0° (normal incidence), 15°, 30°, and 45° can selectively detect fluorescence from both epithelial and stromal layers of epithelial tissue and provide a sensitivity range that is superior to that achieved with the multiseparation approach.<sup>7</sup> In this Letter the findings from a subset of the Monte Carlo simulations are verified by use of two-layered tissue phantoms of epithelial tissue. Our main goals are to show the feasibility of building an angled illumination probe and to demonstrate experimentally the angled probe geometry for depth-sensitive fluorescence spectroscopy of a two-layered turbid medium.

We fabricated a first-generation angled fiber-optic probe in our lab. This angled probe consisted of a central collection fiber, which was fixed perpendicularly to the tissue surface, and two illumination fibers at a subset of illumination angles evaluated in the simulations. These illumination angles were 15°

and 45° relative to the axis perpendicular to tissue surface, and the illumination fibers were placed on the opposite sides of the collection fiber. All fiber tips were polished to be flush with the tip of the probe. All fibers had a core diameter of 200  $\mu\text{m}$  and a numerical aperture of 0.22. The center-to-center distance between the illumination and collection fibers at both illumination angles was approximately 450  $\mu\text{m}$ . Illumination fibers for normal incidence and for an illumination angle of 30° were not included in the angled probe because sensitivity to the epithelial layer is similar for the 0° (normal incidence), 15°, and 30° angles of illumination at illumination-collection fiber separations greater than 400  $\mu\text{m}$ .<sup>7</sup>

The illumination fibers of the probe were coupled to an argon-ion laser (Innova 305 C, Coherent, Inc., Santa Clara, Calif.), which provided a maximum power of 0.19 W at 351 nm. The output power from the laser was attenuated to 1.90 mW by an adjustable aperture and a neutral-density filter and then coupled into the angled illumination fiber. The actual output powers of the illumination fibers were measured by a calibrated optical powermeter and were found to be approximately 650 and 300  $\mu\text{W}$  for illumination angles of 15° and 45°, respectively. The collection fiber of the probe was coupled to the detection module of a fluorophotometer (Skinscan, J. Y. Horiba, Inc., Edison, N.J.), which comprises double emission scanning monochromators and a photomultiplier tube (PMT).

Two-layered agar phantoms were made to mimic human epithelial tissues based on previously published recipes.<sup>5</sup> The thickness of the top layer was varied from 300 to 900  $\mu\text{m}$  in 300- $\mu\text{m}$  increments to cover the range of thicknesses of human epithelium,<sup>1-4</sup> whereas that of the second layer and the lateral dimension were set at a large value ( $\geq 1$  cm) to represent a semi-infinite medium. Plastic wraps ( $\sim 10$   $\mu\text{m}$  in thickness) were placed between the two layers as well as between the probe tip and the top layer to prevent diffusion of phantom components. In the top layer, scattering was achieved with a suspension of polystyrene spheres (diameter of particles, 1.053  $\mu\text{m}$ ) at a concentration of 0.266% by volume (Polysciences, Inc., Warrington,

**Table 1. Values of  $\mu_a$  [ $\text{cm}^{-1}$ ],  $\mu_s$  [ $\text{cm}^{-1}$ ], and  $g$  (left to right) for the Top and Bottom Layers of the Two-Layered Phantom at the Excitation Wavelength and at the Peak Emission Wavelengths of NADH and Rhodamine B**

Layer	Wavelength (nm)		
	351	460 (NADH)	580 (Rhodamine B)
Top	4.2, 118.5, 0.91	3.0, 132.1, 0.91	2.2, 113.9, 0.91
Bottom	22.4, 331.8, 0.91	7.4, 369.9, 0.91	3.8, 318.9, 0.91

Pa.). Absorption was achieved by addition of ink (Super Black India ink; Speedball Art Products Company, Statesville, N.C.) at a concentration of 0.46% by volume. An endogenous fluorophore, NADH, with a fluorescence emission maximum at 460 nm ( $\beta$ -NADH; Sigma Chemical Company, St. Louis, Mo.) was added at a concentration of 0.395 mM. The bottom layer was composed of a polystyrene sphere suspension at a concentration of 0.745% by volume, and an absorber, hemoglobin (product H7379, human hemoglobin; Sigma Chemical Company) at a concentration of 93  $\mu\text{M}$ . An organic dye, Rhodamine B (Sigma Chemical Company) with a fluorescence emission maximum at 580 nm was added at a concentration of 1.044 mM.

The reason for using ink as the absorber in the top layer of the phantom is that the ratios of the absorption coefficient of ink at the excitation wavelength to those at the peak emission wavelengths of 460 nm (peak fluorescence emission of NADH) and 580 nm (peak fluorescence emission of Rhodamine B) are similar to those reported in the literature for the epithelium.<sup>8</sup> The reason for using hemoglobin as the absorber in the bottom layer is that it is the primary endogenous chromophore in the stroma of epithelial tissues. The absorption coefficients of ink and hemoglobin were measured as a function of wavelength by an absorption spectrophotometer and calculated by Beer's law for defined concentrations. We used Mie theory to calculate the theoretical scattering coefficient and anisotropy factor as a function of wavelength of the polystyrene spheres. The refractive indices used in the Mie theory calculation were 1.6 for the polystyrene spheres (provided by the manufacturer) and 1.33 for water. Table 1 lists the values of the absorption coefficient ( $\mu_a$ ), the scattering coefficient ( $\mu_s$ ), and the anisotropy factor ( $g$ ) for the top and bottom layers of the two-layered phantom at the excitation and peak emission wavelengths of NADH and Rhodamine B. NADH and Rhodamine B were selected as the fluorophores for the top and bottom layers because their nonoverlapping emission spectra facilitate discrimination of the fluorescence that originates from the top and bottom layers. The concentrations of the two fluorophores were chosen such that the two peak emission intensities were within the same order of magnitude.

Figure 1 shows the fluorescence spectra measured from two-layered phantoms with top layer thicknesses of 300, 600, and 900  $\mu\text{m}$ . The fluorescence intensity measured at each illumination angle from the two-layered phantom was divided by the peak fluorescence intensity measured from a Rhodamine B standard (peak excitation and emission wavelength pair of

351–580 nm) by use of the same geometry to account for the differences in the incident power at two angles of illumination. It is obvious that the fluorescence intensities detected at an illumination angle of 45° are at least one order of magnitude higher than those measured at an illumination angle of 15°, regardless of the top layer thickness. This trend is consistent with the results of previous Monte Carlo simulations.<sup>7</sup> Another trend worth noting is that the ratio between the peak intensities at 467 nm (NADH fluorescence in the top layer) and 580 nm (Rhodamine B fluorescence in the bottom layer) is noticeably greater at an illumination angle of 45° than at 15° for top layer thicknesses of 300 and 600  $\mu\text{m}$ . These results suggest that relatively more fluorescence is collected from the top layer when a 45° illumination angle is used.

Figure 2 shows the ratio between the peak intensities at 467 nm (NADH fluorescence in the top layer) and 580 nm (Rhodamine B fluorescence in the bottom layer) for top layer thicknesses of 300, 600, and 900  $\mu\text{m}$ . Results are shown for two phantoms made according to the same recipe. The peak intensity ratio increases as the thickness of the top layer increases, which makes intuitive sense. The most important finding, however, is that the peak intensity ratio at an illumination angle of 45° is greater than that at an illumination angle of 15° when the thickness of the top layer is 300 or 600  $\mu\text{m}$ . These results clearly demonstrate that the angled probe detects fluorescence from the top layer more efficiently at the 45° illumination angle than at the 15° illumination angle. When the thickness of the top layer is 900  $\mu\text{m}$ , the

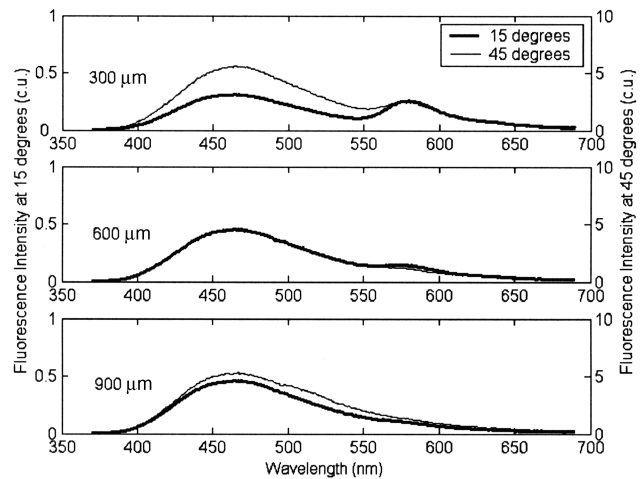


**Fig. 1. Fluorescence spectra measured from two-layered phantoms with top layer thicknesses of 300, 600, and 900  $\mu\text{m}$ ; c.u., calibrated units.**

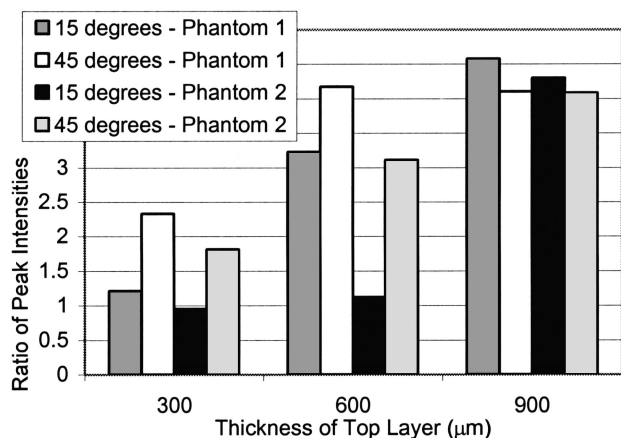


Fig. 2. Ratio between peak intensities at 467 nm (NADH fluorescence in the top layer) and 580 nm (Rhodamine B fluorescence in the bottom layer) for top layer thicknesses of 300, 600, and 900  $\mu\text{m}$ . Results are shown for two phantoms made according to the same recipe.

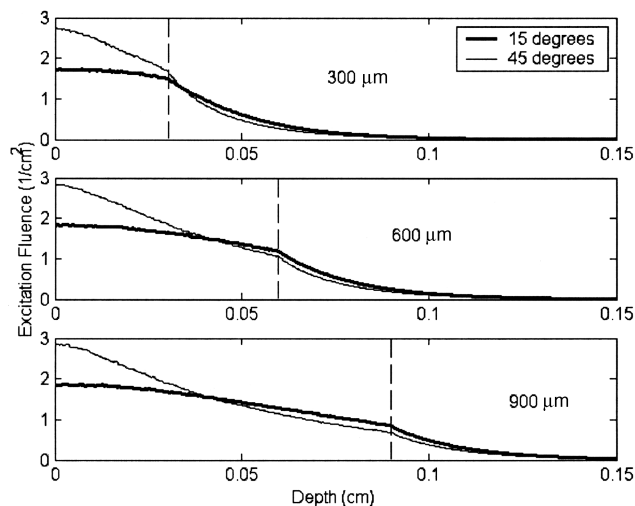


Fig. 3. Simulated excitation fluence as a function of depth for top layer thicknesses of 300, 600, and 900  $\mu\text{m}$  in a theoretical model of the two-layered phantom. Dashed lines indicate the interface between top and bottom layers.

peak intensity ratios at the two illumination angles are similar, suggesting that the maximum depth from which the detected fluorescence originates at both illumination angles is within 900  $\mu\text{m}$ .

To elucidate the underlying basis of the above findings we determined the excitation fluence distribution within the two-layered phantom from Monte Carlo simulations<sup>9</sup> for the 15° and 45° angled illumination geometries. The fluence [ $\text{cm}^{-2}$ ] refers to the radiant energy propagating in all directions through a given location and was calculated by division of the photon energy deposited within a local volume by the local absorption coefficient,<sup>9</sup> which essentially reflects the distribution of excitation light inside this tissue. Figure 3 shows the simulated excitation fluence as a function of depth for top layer thicknesses of 300, 600, and 900  $\mu\text{m}$  in a theoretical model of the two-layered phantom, which provides insight into the basis for depth-sensitive fluorescence detection with the angled illumination probe geometry. Because fluorescence

starts with absorption of excitation light, the distribution of excitation light in the tissue determines where the fluorescence originates. The shallower the distribution of excitation light, the shallower the volume from which the detected fluorescence originates. According to Fig. 3, the distribution of excitation light in the tissue phantom is confined to a more superficial tissue volume as the angle of illumination is increased. Thus it can be inferred that the detected fluorescence also originates from a more superficial volume as the angle of illumination is increased, which leads to two important conclusions: (1) The sensitivity to the fluorescence from the top layer increases with increasing angle of illumination and (2) the detected fluorescence signal increases with increasing angle of illumination because of decreased photon attenuation. These conclusions are expected to be true even when there is a difference between the excitation and the emission wavelength's optical properties because the distribution of excitation light in tissue is determined only by the illumination geometry and optical properties of the phantom at the excitation wavelength.

In this Letter we have experimentally demonstrated depth-sensitive detection of fluorescence from a two-layered turbid medium by using an angled illumination probe. A more-sophisticated angled probe that includes additional angles of illumination (at a smaller separation of 250  $\mu\text{m}$ ) is being developed by our group. This next-generation probe will be tested systematically on solid phantoms and on epithelial tissues *in vivo*.

The authors acknowledge support from the Prize Fellowship, University of Wisconsin—Madison, and from National Institutes of Health grant PO1 CA082710 05. The e-mail address of Q. Liu is qliu@cae.wisc.edu.

## References

1. E. M. Gill, A. Malpica, R. E. Alford, A. R. Nath, M. Follen, R. R. Richards-Kortum, and N. Ramanujam, *Photochem. Photobiol.* **77**, 653 (2003).
2. C. Brookner, U. Utzinger, M. Follen, R. Richards-Kortum, D. Cox, and E. N. Atkinson, *J. Biomed. Opt.* **8**, 479 (2003).
3. I. Pavlova, K. Sokolov, R. Drezek, A. Malpica, M. Follen, and R. Richards-Kortum, *Photochem. Photobiol.* **77**, 550 (2003).
4. R. Drezek, C. Brookner, I. Pavlova, I. Boiko, A. Malpica, R. Lotan, M. Follen, and R. Richards-Kortum, *Photochem. Photobiol.* **73**, 636 (2001).
5. T. J. Pfefer, L. S. Matchette, A. M. Ross, and M. N. Ediger, *Opt. Lett.* **28**, 120 (2003).
6. C. Zhu, Q. Liu, and N. Ramanujam, *J. Biomed. Opt.* **8**, 237 (2003).
7. M. C. Skala, G. M. Palmer, C. Zhu, Q. Liu, K. M. Vrotsos, C. L. Marshek-Stone, A. Gendron-Fitzpatrick, and N. Ramanujam, *Lasers Surg. Med.* **34**, 25 (2004).
8. R. Drezek, K. Sokolov, U. Utzinger, I. Boiko, A. Malpica, M. Follen, and R. Richards-Kortum, *J. Biomed. Opt.* **6**, 385 (2001).
9. S. L. Jacques and L. Wang, in *Optical-Thermal Response of Laser-Irradiated Tissue*, A. J. Welch and M. J. C. van Gemert, eds. (Plenum, New York, 1995), pp. 73–100.